Developing software for Processing of Low frequency passive seismic data: A case study of Cambay Basin

Bhanu Pratap Singh, A K Srivastava and K V Krishnan, ONGC, India*
Singh_bhanu1@ongc.co.in

Keywords

Low frequency passive seismic, V/H, PS, Polarization attributes.

Summary

A pilot study has been carried out to establish the efficacy of Low Frequency Passive Seismic (LFPS) survey to locate oil/gas pools in Cambay Basin. The present paper discussed the development of software for processing of LFPS data for deriving various attributes such as spectral analysis, V/H ratio, PSD and various polarization attributes. The anomalous attributes in Jotana area of Cambay Basin correlates well with presence of hydrocarbon in known oil and dry wells.

1. Introduction

In Low Frequency Passive Seismic (LFPS) technique, energy of micro-tremors generated from natural seismicity of the earth is recorded on earth's surface using very high sensitive Low Frequency sensors. Various attributes derived by spectral analysis of LFPS data like, Vertical to Horizontal amplitudes Ratio (V/H), Power Spectral Density (PSD), Peak Frequency Distribution (PFD), polarisation attributes etc. show anomalous response in 1 to 6 Hz range over hydrocarbon reservoir and thus help to estimate the presence of oil/gas pools. It is found that over hydrocarbon pools, V/H ratio of 2-4 Hz micro-tremors indicate values > 1. The processing software for deriving these attributes were developed in Python and using MATLAB.

2. About area:

Cambay Basin was formed during early Cretaceous due to rifting along Dharwarian orogenic trends during northward migration of the Indian plate after its break up from Gondwana land. In the early stages of rift, the primodial lineaments reactivated. The rift-drift transition phase of Indian plate witnessed volcanic events in Cambay Basin during K/T times and represented by widespread Deccan trap. Subsequent rift & drift lead to creation of undulating Basin floors with highs and Lows providing depocentres for huge thickness of sediments. Olpads derived from erosion of Deccan traps correspond to early synrift phase of Basin evolution. The extensional architecture of the basin is defined by two types of faults viz., 'listric normal faults', striking N-S to NNW-SSE and 'transfer faults', trending ENE-WSW to NE-SW. The listric faults mostly run sub parallel to the rift - border faults. Transfer faults frequently offset the listric faults. Thus basin architecture is defined by an enechelon arrangement of asymmetric half grabens bordered by listric normal faults oblique to the rift axis and are separated by transfer fault zones/accommodation zones and basement highs. A thick sequence of sedimentary rocks ranging in the age from Paleocene to Recent overlies the Deccan Trap, which is considered as technical basement in Cambay Basin. The overlying sedimentary sections from deeper to shallower consist of Olpad, Older Cambay shale, Kadi, Kalol, Tarapur shale and other younger sequences. Kadi Formation is further differentiated into Chhatral, Mehsana and Mandhali members. Kadi Formation progressively thins away from Basin axis & ultimately they wedge out against Mehsana Horst in the west and Basin margin faults in the east. During Late Miocene, few areas in the basin experienced inversion tectonics related to Himalayan Orogeny.
The major oil fields in this area are Lanwa-Santhal-Balol producing exclusively from Kalol Formation whereas Jotana, North-Kadi, Sobhasan, Linch and Nandasan fields produce from multiple plays ranging from Older Cambay shale to Kadi and Kalol Formations. Exploration has reached a mature stage and at present it is focused on subtle traps and small amplitude entrapment situations in the areas bordering established fields. The general stratigraphy is shown in figure 1.

3. Jotana Field:

Jotana field was discovered in 1977 & put on production since 1980. It is a major fault built structure, measuring 17 Kms in length and 3 Kms in width.

Developing software for Processing of Low frequency passive seismic data: A case study of Cambay Basin

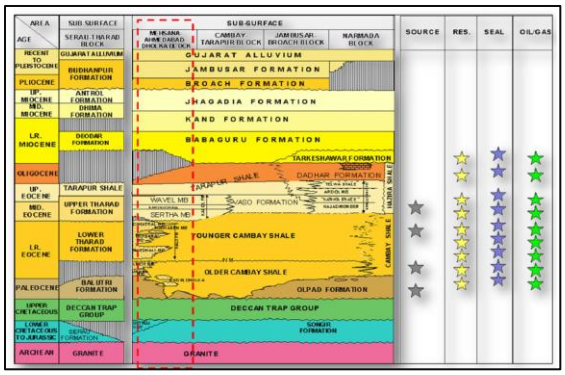

Figure 1. General stratigraphy

It is a multi-layered reservoir within Linch, Mandhali, Mehsana & Kalol formation of Eocene age in the chronological order. These reservoirs have a high degree of vertico-lateral heterogeneity. The combinational trap is characterized by the presence of transverse faults which have compartmentalized the multiple layered oil and gas reservoirs in numerous small-sized pools. Major producers are Mandhali and BCSS sands. The field is highly complex having 41 pay zones distributed over 258 blocks due to faulting, pinching/wedging out of the pay sands and different OWC and OSC.

Some of the blocks, separated by transverse faults, are communicating across the faults and fault juxtaposition. Sand deposition has generally taken place as distributary channel system from North & North-East and as mouth bar in the South in a tidal dominated delta system.

Kalol sands are aquifer supported reservoirs having a bottom water drive. BCSS sands are having edge water drive as well as bottom water drive.

Mandhali member of Kadi formation constitutes about 76% of the OIIP and comprises of three major sequences, namely MU-I, MU-II & MU-III separated by maximum flooding surfaces. These three layers are further divided into 24 sub units separated by shale in between.

There are two massive coal units one just below the Kalol sands termed as top coal with a thickness variation of around 10-15 meters, underlaid by sand units named as BTCS which are further underlaid by bottom coal with a thickness variation of 20-35 meters.

Although ONGC has acquired the seismic data over the Jotana field and the adjoining area extensively. The thick Mehsana coal acts as the barrier in the energy penetration below it. The energy loss due to thick coal, pinching out the events results in non-discernable of seismic events.

A pilot study has been carried out to establish the efficacy of Low Frequency Passive Seismic (LFPS) survey to locate oil/gas pools in Jotana area of Cambay Basin as shown in figure 2. The processing of the LFPS data were attempted using Python and MATLAB Software.

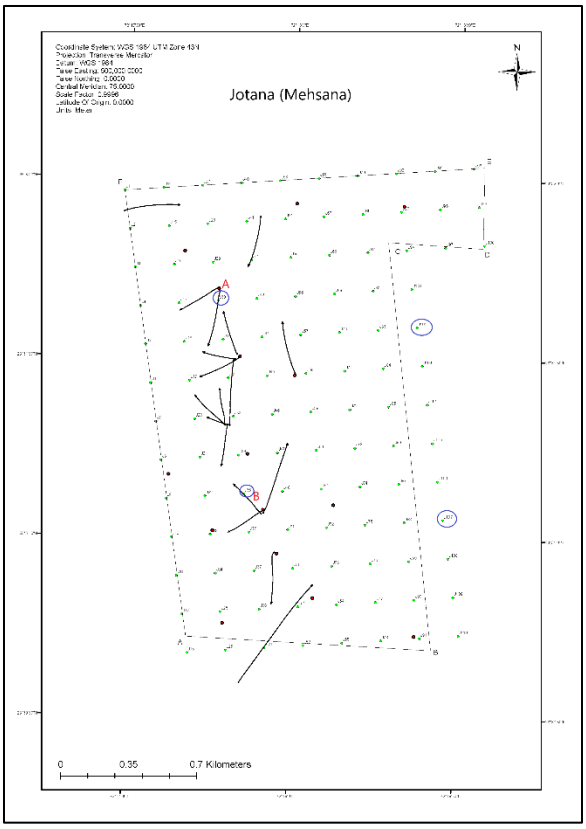

Figure 2. Oil/Gas pools and location of stations in Jotana area of Cambay Basin.

4. Development of Processing Steps

MATLAB software is being used to visualize the data. The three component data is first loaded and read. Time series and amplitude spectrum of all the three components are plotted. A band pass filter is applied to the input data with a low cut frequency of 0.05 Hz and a high cut frequency of 10 Hz. The time series of all the three components of the filtered data is plotted and the spikes which still remain are manually selected using the ginput() utility of the

Developing software for Processing of Low frequency passive seismic data: A case study of Cambay Basin

MATLAB software. The samples in the raw data which corresponds to the selected spikes are then removed from the three component input data and the time series and frequency spectrum of the cleaned data are again plotted. The cleaned data is divided into 20 seconds windows with 50% overlapping. A cosine tapering of 10% is applied to all the windows to account for spectral leakage. Fourier transform of all the windows is taken and averaged to form a single window for each components. The frequency axis is being prepared. The V/H ratio is then calculated as follows:

$$vh = \frac{zm}{\sqrt{\frac{xm^2 + ym^2}{2}}}$$

Where xm and ym are the mean of x and y components, respectively, and zm is the mean of the z (vertical) component. The V/H ratio thus obtained is smoothed using the Konno-Ohmachi Algorithm, with bandwidth coefficient, b = 40. V/H ratio is plotted against frequency. Peak value of V/H in the frequency range of 2-5Hz and the corresponding frequency is captured. Polarization attributes are developed for further analysis of strength, orientation and variation of passive seismic wavefield.

In the Jotana area of Gujrat, an LFPS sensor was placed at station J30 (stations circled in blue in Figure 2) near an oil producing well A. Another sensor was placed at station J35 near a deviated oil producing well B. Data was recorded for 12 hours, sampled at a frequency of 128 Hz. Time series and the respective amplitude spectrum of the three component data was plotted.

A band pass filter with a low cut frequency of 0.05Hz and a high cut frequency of 10Hz was then applied to all the three components and the time series thus obtained was observed, as shown in figure 3. As too many spikes were still visible, manual selection of spikes was not performed and surgical mute was not done. Therefore, the raw data of 12 hours was used as it is. The data was divided into 50% overlapping windows of 20 seconds each and 10% cosine tapering applied. Fourier transform of all the windows was taken using the fast fourier transform utility provided in matlab. A single window was obtained for each of the three components by averaging the corresponding fft points of all the windows.

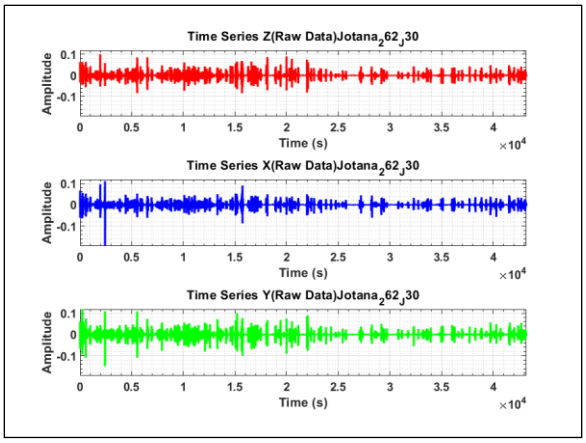

Figure 3. Time Series of raw input at station J30

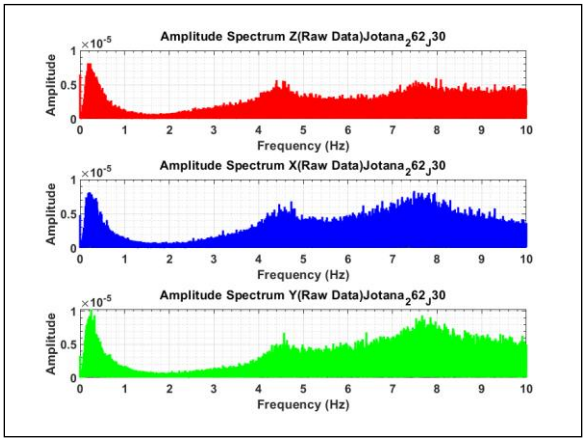

Figure 4. Amplitude Spectrum of raw input at station J30

The V/H Ratio was calculated using the below equation:

$$vh = \frac{zm}{\sqrt{\frac{xm^2 + ym^2}{2}}}$$

Where,
zm = mean fourier trasnform, z (vertical)
xm = mean fourier transform, x (N-S)
ym = mean fourier transform, y (E-W)

The V/H ratio was then smoothed using the Konno-Ohmachi algorithm, with bandwidth coefficient, b=40.

Power spectral density curve was also plotted for the two stations J30 and J35. PSD curve shows the variations of energy as a function of frequency.

Developing software for Processing of Low frequency passive seismic data: A case study of Cambay Basin

Similar to the V/H response, the PSD curve shows a peak in the frequency range of 1-6 Hz. For station J30 (figure 7) and station J35 (figure 13), which are placed near oil bearing wells, the PSD curve shows a higher peak in the frequency range of 1-6 Hz.

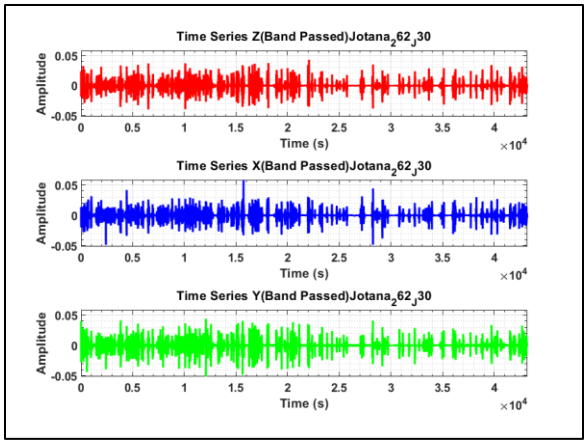

Figure 5. Time Series after applying the Band pass filter (lc = 0.05 Hz, hc = 10 Hz). A lots of spikes are still visible. Surgical mute thus not performed.

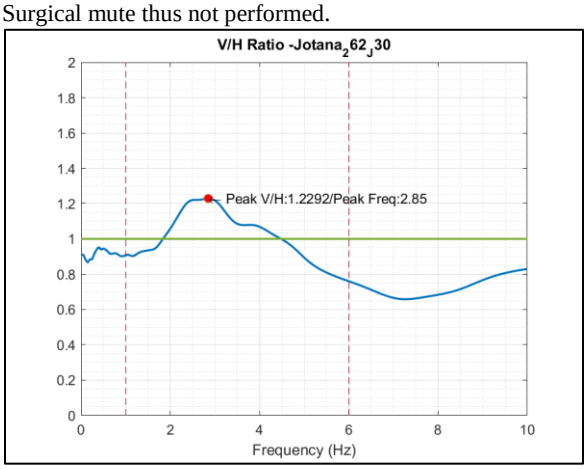

Figure 6. V/H Ratio, station J30. Peak shown at 2.85 Hz (in 2-5Hz range). V/H=1.2292.

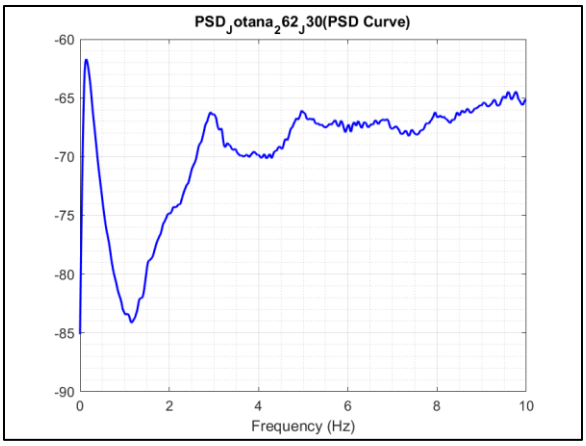

Figure 7. PSD Curve for station, J30.

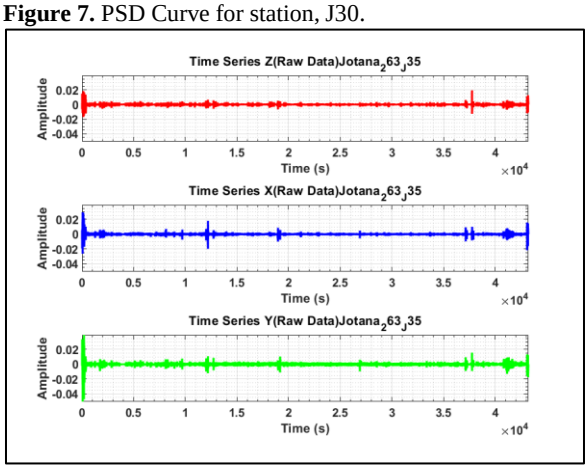

Figure 8. Time series of raw input data, J35.

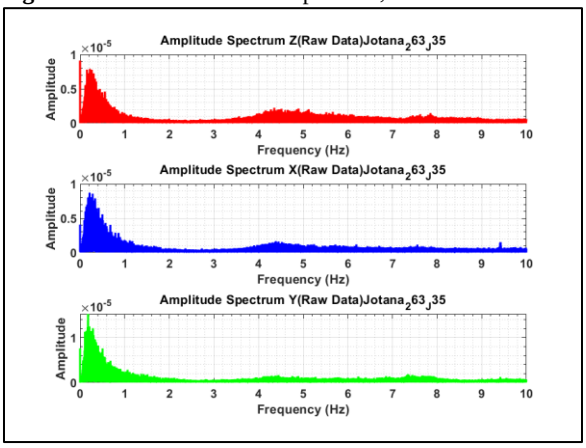

Figure 9. Amplitude spectrum of raw data, J35.

Developing software for Processing of Low frequency passive seismic data: A case study of Cambay Basin

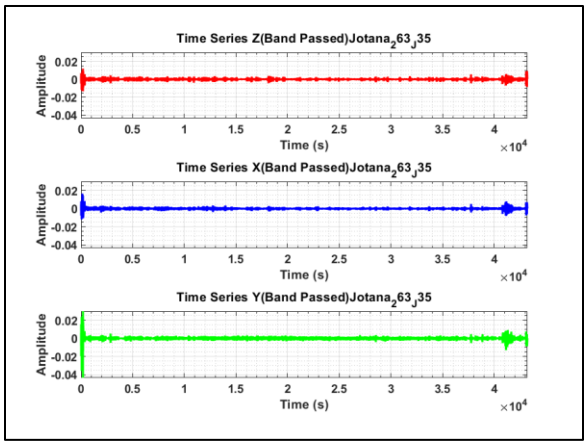

Figure 10. Time series after the band pass filter applied, station J35. The portion in the figure showing the spikes indicate noisy data. The portion corresponding to the spikes in the raw data was surgically muted by manually removing that portion from the raw data.

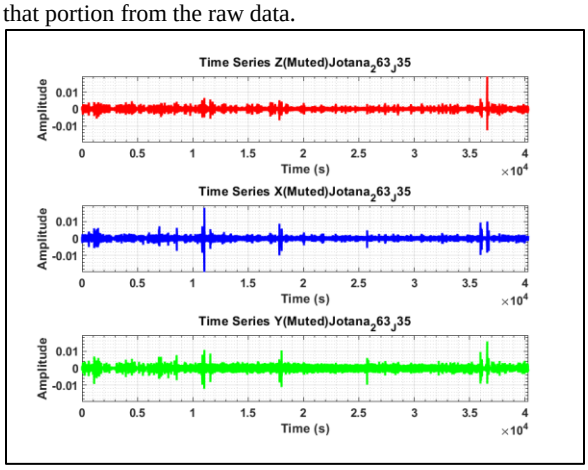

Figure 11. Time series after removing the noisy portions in the raw input, station J35.

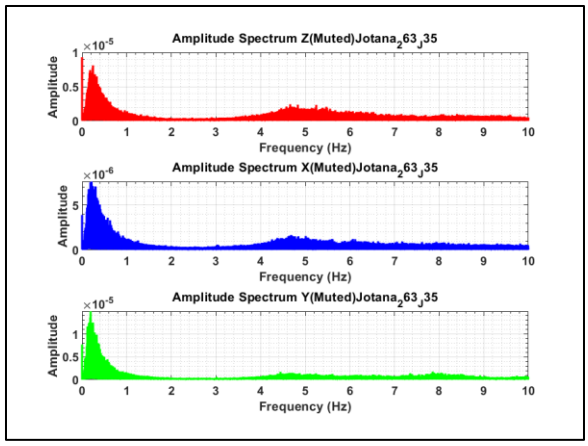

Figure 12. Amplitude spectrum after removing the noisy portions in the raw input, station J35.

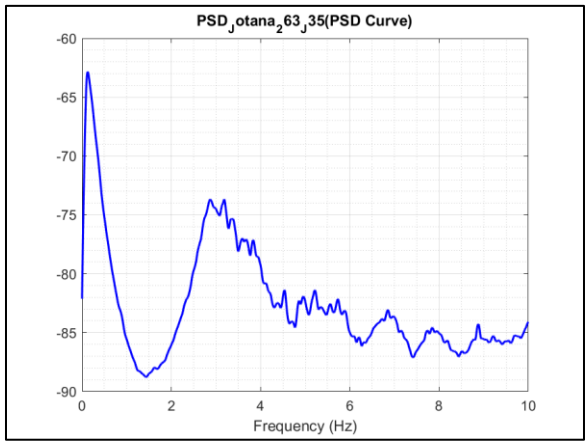

Figure 13. PSD Curve for station J35.

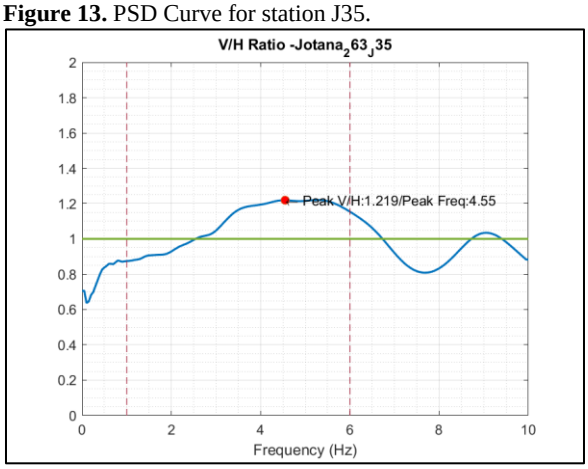

Figure 14. V/H Ratio, station J35. Peak shown at 4.55 Hz (in 2-5Hz range). V/H=1.219.

Developing software for Processing of Low frequency passive seismic data: A case study of Cambay Basin

The processing steps that were followed for station J30 were similarly applied for the data recorded by the station J35 located in close proximity of oil producing well B. Figure 8 to figure 14 shows to outputs at various stages for station J35.

Two stations J107 and J102 were placed in dry zones far away from the oil bearing wells (as shown in blue circles in Figure 2). Similar processing steps were performed on the data provided by these two stations. The V/H graphs for the two are shown in figure 15 and figure 16, respectively. PSD Curve for the two are shown in figure 17 and figure 18. PSD curve for both the stations show lower peaks and is on a decreasing trend

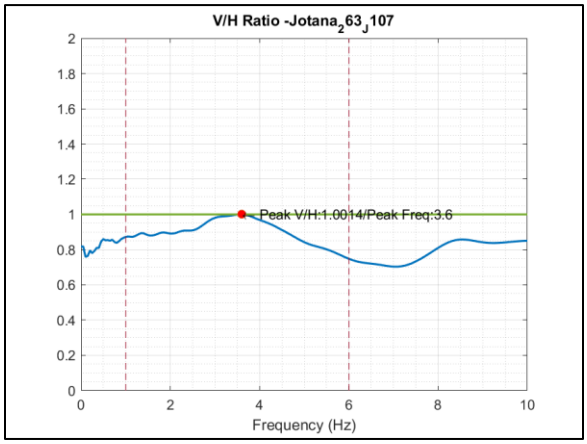

Figure 15. V/H ratio for station J107. (V/H = 1.0014). The V/H ratio is not more than 1 in the frequency range of 1-6Hz.

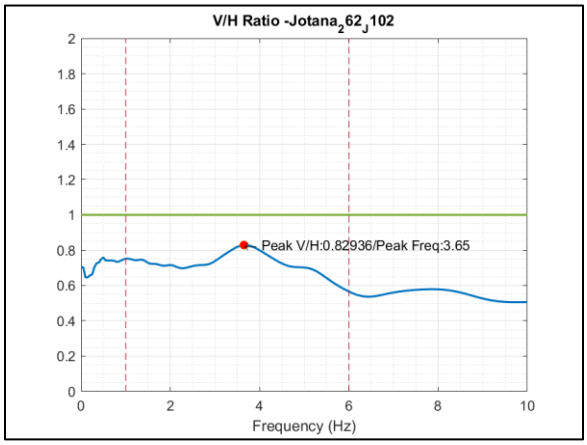

Figure 16. V/H ratio for station J102. (V/H = 0.82396). The V/H ratio is less than 1 in the frequency range of 1-6Hz.

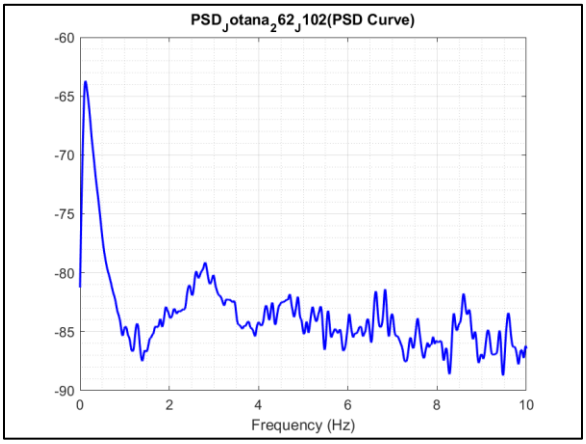

Figure 17. PSD Curve for station J102.

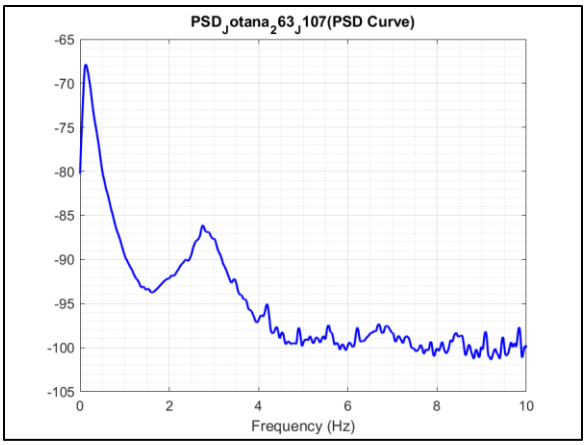

Figure 18. PSD Curve for station J107.

Out of the four stations, two stations which were placed in close proximity to an oil bearing well showed V/H values greater than 1 and a higher PSD curve in 1-6Hz frequency range. However, the other two stations placed in a dry zone showed a V/H value less than 1 in the same frequency range. Similar observations are visible when the PSD curves of the four stations are compared. These observations provide conclusive evidence that V/H ratio and PSD curve estimates play an important role in establishing presence of hydrocarbons in an area.

5. Polarization Attributes

Developing software for Processing of Low frequency passive seismic data: A case study of Cambay Basin

A band pass filter is applied to the N length 3 component (X, Y, Z) data that passes the frequencies from 1 to 6 Hz. A 3x3 covariance matrix is prepared as:

$$C = \begin{bmatrix} C_{xx} & C_{xy} & C_{xz} \\ C_{xy} & C_{yy} & C_{yz} \\ C_{xz} & C_{yz} & C_{zz} \end{bmatrix}$$

Where,

$$C_{xx} = \sum_{i=1}^{N} (X_i - \bar{X})^2$$

$$C_{xy} = \sum_{i=1}^{N} (X_i - \bar{X})(Y_i - \bar{Y})$$

$$C_{yz} = \sum_{i=1}^{N} (Y_i - \bar{Y})(Z_i - \bar{Z})$$

$$C_{yy} = \sum_{i=1}^{N} (Y_i - \bar{Y})^2$$

$$C_{zz} = \sum_{i=1}^{N} (Z_i - \bar{Z})^2$$

Using the covariance matrix, the eigenvectors and eigenvalues are calculated using the eig() utility of MATLAB. The three eigenvalues returned are λ_1, λ_2 and λ_3, with λ_1 being the largest eigenvalue, referred to as the strength of the signal.

The rectilinearity parameter L, sometimes called linearity, relates the magnitude of the intermediate and smallest eigenvalue to the largest eigenvalue.

$$L = 1 - \left(\frac{\lambda_2 + \lambda_3}{2\lambda_1}\right)$$

It measures the degree of how the linear incoming wave field is polarized. It yields value between zero and one. Zero being random and one being linearly directed. Azimuth and dip are also calculated. They describe the orientation of the largest eigenvector, $p_1 = (p_1(x), p_1(y), p_1(z))$.

The dip is calculated as

$$\phi = arctan\left(\frac{p_{1(z)}}{\sqrt{p_{1(x)^2} + p_{1(y)^2}}}\right)$$

It is zero for a horizontal polarization and is defined positive for the positive z-direction. The azimuth is specified as

$$\theta = arctan\left(\frac{p_{1(y)}}{p_{1(x)}}\right)$$

and is measured counterclockwise from the positive x-axis. Strength variations of the signal, largest eigenvalue, λ_1, was also analyzed and plotted for all the four stations.

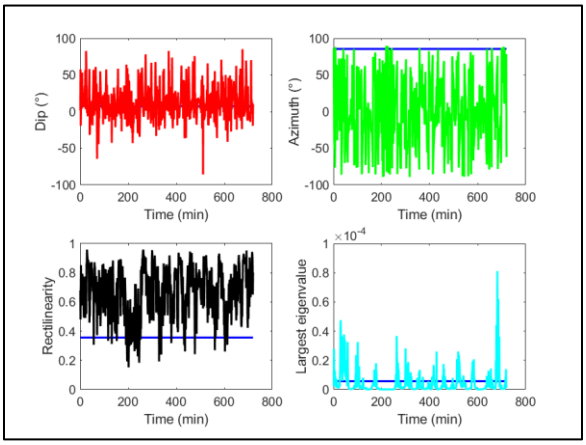

Figure 19. Time variations of four polarization attributes for station J30. The horizontal solid line represents the value using data of the whole time period.

Time intervals of 60 s are analyzed. The horizontal solid blue line represents the value using the data of the whole time period. A dip of ϕ = 90° indicates vertical plane oscillation and an azimuth of Θ = 0° indicates north-south particle oscillation.

Developing software for Processing of Low frequency passive seismic data: A case study of Cambay Basin

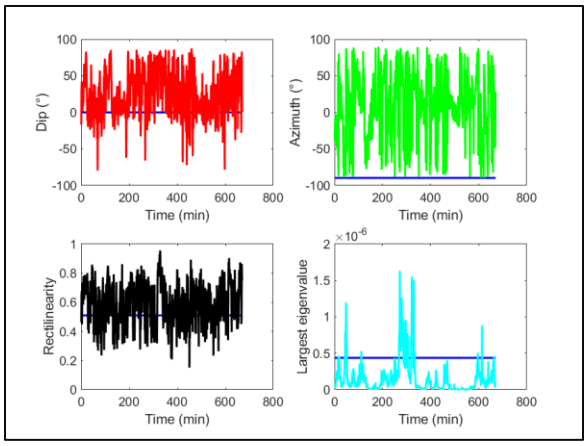

Figure 20. Time variations of four polarization attributes for station J35.

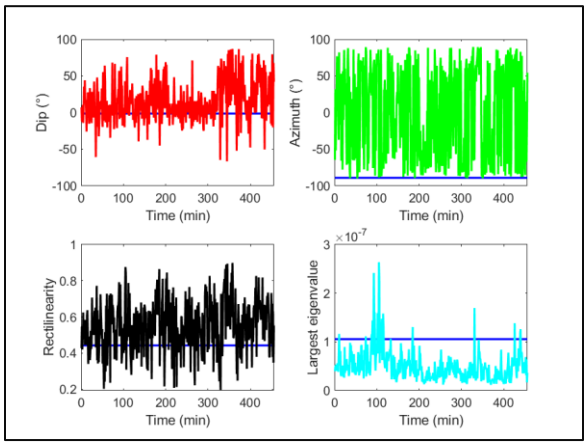

Figure 21. Time variations of four polarization attributes for station J107.

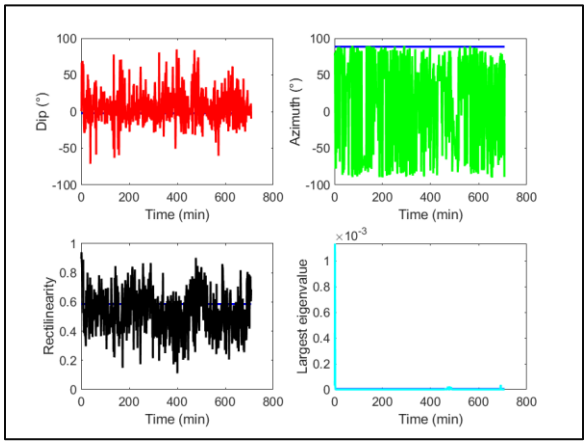

Figure 22. Time variations of four polarization attributes for station J102.

As per Saenger Et Al (2009), the following table summarizes the polarization attributes with respect to the PSD curve.

Attributes	**Hydrocarbon Location**	**Non-Hydrocarbon Location**
Dip ϕ	Stable, high value	Stable, low value
Azimuth θ	Unstable	Relatively stable
Largest Eigenvalue λ_1	Varying, but relatively high	Relatively low with some spikes
Rectilinearity L	Relatively high, relatively stable	Relatively lower

Table 1. Comparison of polarization attributes.

Attr	**J30**	**J35**	**J102**	**J107**
Dip ϕ	Low	High	Low	Low
Azimuth θ	Unstable	Unstable	Unstable	Unstable
Largest Eigenvalue λ_1	Relatively low with spikes	Relatively high with spikes	High without spikes	Low with spikes
Rectilinearity L	Relatively high	Relatively high	Relatively Low	Relatively high

Table 2. Observations made for the four stations.

6. Conclusion

Based on the analysis and work flow adopted for processing of LFPS data, the V/H attribute provides a distinct anomaly over hydrocarbon reservoir and thus helps to estimate the presence of hydrocarbons. Study of the polarisation attributes is useful for further analysis of passive seismic wavefields. Station J35 with a higher PSD curve, also shows a higher dip and relatively higher rectilinearity. Similary, station J102 with a decreasing PSD curve shows a lower rectilinearity. Station J35, thus provides better estimates for hydrocarbon presence.

7. Acknowledgement

Developing software for Processing of Low frequency passive seismic data: A case study of Cambay Basin

Authors are grateful to Oil and Natural Gas Corporation Limited, India for providing the necessary facilities to carry out this work.
Authors are grateful to Shri R K Srivastava, Director (Exploration) ONGC for his permission to publish this paper.
The authors are thankful to Dr. M Ravikumar, Director General ISR, Gandhinagar and his team for providing help in data acquisition.
The authors are thankful to the members of processing team who have directly or indirectly contributed in completion of the project.
The views expressed in this paper are those of authors only and do not necessarily reflect their employer's opinion.

8. References

Al-khalifah, T. and Tsvankin, I., 1995, Velocity analysis for transversely isotropic media; Geophysics, 60, 150-1556.
Backus, G. E., 1962, Long-wave elastic anisotropy produced by horizontal layering; J. Geophysical Res., 67, 4427-4440.
Thomson, L., 1986, Weak elastic anisotropy; Geophysics, 51, 1954-1966.
Erik H. Saenger, Stefan M. Schmalholz, Marc-A. Lambert, Tung T. Nguyen, Arnaud Torres, Sabrina Metzger, Robert M. Habiger, Tamara Müller, Susanne Rentsch, and Efraín Méndez-Hernández, (2009), "A passive seismic survey over a gas field: Analysis of low-frequency anomalies," GEOPHYSICS 74: O29-O40.
Ebrahimi, Mostafa & Moradi, Ali & Seidin, Hamid. (2018). Analysis of Low-Frequency Passive Seismic Attributes in Maroun Oil Field, Iran. Journal of the Earth and Space Physics. 43. 11-26. 10.22059/jesphys.2017.216290.1006846.
K. Konno & T. Ohmachi (1998) "Ground-motion characteristics estimated from spectral ratio between horizontal and vertical components of microtremor." Bulletin of the Seismological Society of America. Vol.88, No.1, 228-241.